Investigations of SO 4 2– adsorption at the Au(111) electrode by chronocoulometry and radiochemistry. J Electroanal Chem

ARTICLE *in* JOURNAL OF ELECTROANALYTICAL CHEMISTRY · MARCH 1994

Impact Factor: 2.73 · DOI: 10.1016/0022-0728(93)03008-D

Investigations of SO_4^{2-} adsorption at the Au(111) electrode by chronocoulometry and radiochemistry *

Z. Shi and J. Lipkowski

Guelph–Waterloo Centre for Graduate Work in Chemistry, Guelph Campus, University of Guelph, Guelph, ON N1G 2W1 (Canada)

M. Gamboa, P. Zelenay and A. Wieckowski

Department of Chemistry, University of Illinois, 1209 W. California St., Urbana, IL 61801 (USA)

Received 6 May 1993; in revised form 24 June 1993

Abstract

Chronocoulometry was employed to measure charge density at the Au(111) electrode surface. Thermodynamic analysis of the charge density data for ionic adsorption from a solution with an excess of a supporting electrolyte is described and used to study SO_4^{2-} adsorption at the Au(111) electrode from a 0.1 M $HClO_4$ solution. The Gibbs excesses determined from the charge density data are compared with the Gibbs excesses determined from radiochemical measurements using ^{35}S-labelled sulphate solutions. Very good agreement between the Gibbs excesses determined by the two techniques is observed.

Essin–Markov coefficients for SO_4^{2-} adsorption from two series of solutions were determined: (i) at constant pH and variable K_2SO_4 concentration; (ii) at constant K_2SO_4 concentration and variable pH. The Essin–Markov coefficients were used to identify the nature of the adsorbed species (HSO_4^- or SO_4^{2-}). Our results indicate that SO_4^{2-} ion is the adsorbed species even if HSO_4^- predominates in the bulk of the solution.

1. Introduction

This is the second paper in which the measurements of the Gibbs excesses determined by the radiochemical technique and from the thermodynamic analysis of chronocoulometric data are compared. In the first contribution the investigations of the adsorption of a neutral organic molecule were discussed [1]. In this paper the adsorption of the sulphate ion at the Au(111) electrode is described and the strengths and limitations of the two techniques for the study of ionic adsorption at solid electrodes are discussed.

There is much interest in the adsorption of SO_4^{2-} at gold electrodes owing to efforts to understand either the structure of the metal–solution interface [2–8] or to explain the role of SO_4^{2-} adsorption in the copper underpotential deposition at gold electrodes [9–13]. The qualitative features of SO_4^{2-} adsorption at Au electrodes were described with the help of cyclic voltammetry [4,5]. However, with the exception of a recent paper by Zelenay et al. [6] for polycrystalline Au, the quantitative data for SO_4^{2-} adsorption at gold electrodes are lacking. In fact, the first Gibbs excesses for SO_4^{2-} adsorption at the surface of an Au(111) single-crystal electrode are reported here.

2. Experimental

All electrochemical experiments were performed using a gold single-crystal electrode prepared by flame annealing as described elsewhere [14,15]. The counter-electrode (CE) was a gold coil cleaned by flame annealing. The reference electrode (RE) was a saturated calomel electrode (SCE) connected to the supporting electrolyte through a salt bridge.

Water was purified in a Millipore system (> 17 MΩ cm). The supporting electrolyte was either 0.05 M $KClO_4$ + 0.02 M $HClO_4$ or 0.1 M $HClO_4$. Potassium perchlorate was purified as described previously [14]

* Dedicated to Professor J.H. Sluyters on the occasion of his retirement from the University of Utrecht and in recognition of his contribution to electrochemistry.

0022-0728/94/$7.00
SSDI 0022-0728(93)03008-D

and, perchloric acid (Aldrich Chemical Company, redistilled, 99.999%) was used without further purification. The supporting electrolyte was purged with argon to remove oxygen.

The radiochemical experiments were performed using a gold single-crystal electrode (Johnson and Matthey, 99.995% purity) polished and cleaned according to the procedure described in ref. [6]. The electrode was flame annealed before each experiment. The measurements were conducted in a glass–Teflon cell equipped with a gold CE and a Ag/AgCl reference electrode ($[Cl^-] = 1$ M). For comparison with the electrochemical results the potentials measured in the radiochemical experiments were converted to the SCE scale. They are reported versus SCE in this paper. The ^{35}S-labelled sulphate was supplied by Amersham and its specific activity used for measurements was 10 Ci mol^{-1}. A glass scintillator plate was built in the bottom of the cell to measure the radioactivity of the solution and of the surface species. Millipore water was used for solution preparation. Perchloric acid was used as supplied (Mallinckrodt, AR grade). All electrochemical and radiochemical measurements were conducted at room temperature (20 ± 2°C).

2.1. Equipment

The electrochemical experiments were performed using a PAR model 173 potentiostat and a PAR model 5209 lock-in amplifier controlled by a computer. All data were acquired via a plug-in acquisition board (RC Electronics model IS-16). Custom software was used to record cyclic voltammograms (CVs) and differential capacity curves $C(E)$ (5 mV r.m.s., 25.0 Hz ac) and to perform the chronocoulometric experiments. Radiochemical work was conducted using a glass scintillator detector [16] optically coupled to a low dark current photomultiplier tube (Thorn-EMI). Pulse-counting measurements and data acquisition were performed using Ortec electronics and an IBM PC-XT computer, respectively. The Au(111) electrode potential was maintained by a PAR model 171 potentiostat, a PAR model 175 universal programmer and a Hewlett Packard model 1035B x–y recorder.

2.2. Methodology

Cyclic voltammetry and differential capacities were used for qualitative characterization of the electrode surface. Potential-step experiments were performed to obtain quantitative data for the SO_4^{2-} and/or HSO_4^- adsorption. The electrode was initially held at potential E, where SO_4^{2-} and/or HSO_4^- adsorption takes place, for a period of time long enough for the adsorption equilibrium to be established (the solution was stirred if the bulk sulphate concentration was less than 10^{-4} M), and then the potential was stepped to the negative limit E_0 of potentials investigated where the SO_4^{2-} and/or HSO_4^- ions were totally desorbed from the gold surface ($E_0 = -200$ mV/SCE). The current transients resulting from the recharging of the double layer were recorded and subsequently integrated to give the chronocoulometric curves. The primary piece of information, the difference $\Delta\sigma_M$ between the charge densities at E and E_0, was obtained by extrapolating the chronocoulometric curves to time zero. The absolute charge densities σ_M were then calculated from $\Delta\sigma_M$ using the value of the potential of zero charge (pzc) determined independently from differential capacity curves. This procedure was repeated for E covering the whole double-layer region of the gold electrode using a 25 mV increment between each step. In this way the charge density versus potential curves for different bulk SO_4^{2-} concentrations were determined. Two series of experiments were performed in solutions of mixed electrolytes. The first was 0.02 M $HClO_4$ + 0.05 M $KClO_4$ + x M K_2SO_4, and the second was 0.1 M $HClO_4$ + x M K_2SO_4 where the concentration of K_2SO_4 varied between 5×10^{-6} M and 5×10^{-3} M. The charge density curves were then integrated to calculate relative values of the interfacial tension γ. In the present series of measurements the concentration of K_2SO_4 was at least 10 times smaller than the concentration of $HClO_4$ or $KClO_4$. The total concentration of cations and the ionic strength of the solution could then be considered constant (independent of $c_{K_2SO_4}$). Under these conditions the electrocapillary equation can be written as (see Appendix A, eqn. (A12))

$$-d\gamma = \sigma_M \, dE + \Gamma_- RT \, d \ln c_{SO_4^{2-}} \quad (1)$$

where E is the electrode potential measured with respect to SCE and $\Gamma_- = \Gamma_{SO_4^{2-}} + \Gamma_{HSO_4^-}$ is the sum of the Gibbs excesses $\Gamma_{SO_4^{2-}}$ and $\Gamma_{HSO_4^-}$ of SO_4^{2-} and HSO_4^-, respectively. The Gibbs excess Γ_- was therefore calculated by differentiation of plots of the relative interfacial tension versus $\ln c_{SO_4^{2-}}$ at constant E, or by plotting the Parsons function $\xi = \gamma + \sigma_M E$ [17] and differentiating the relative ξ versus $\ln c_{SO_4^{2-}}$ plots at constant σ_M (see Appendix A, eqn. (A13)). The concentration of SO_4^{2-} can be calculated from the total concentration $c_{K_2SO_4}$ of K_2SO_4 in solution and the value of the acid dissociation constant $K_a(HSO_4^-) = 1.2 \times 10^{-2}$ [18]. Alternatively, the Gibbs excess can be determined to a good approximation by differentiating the relative interfacial tension (or relative values of the Parsons function) with respect to the logarithm of the total K_2SO_4 concentration (see Appendix A, eqn. (A9)).

The radiochemical measurements were conducted in 0.1 M $HClO_4$ + 5×10^{-4} M K_2SO_4 solution. During these experiments the electrode was initially held away

from the scintillator window at a potential E at which SO_4^{2-} and/or HSO_4^- adsorbs at the Au(111) surface for a period of time long enough for the adsorption equilibrium to be established (1 min in the 5×10^{-4} M SO_4^{2-} solution). The electrode was then lowered against the scintillator to a distance of approximately 2 μm and the radioactivity counts were measured. Next, a similar experiment was repeated applying a negative potential E_0 at which SO_4^{2-} and/or HSO_4^- ions are desorbed from the electrode surface. The difference between the counts measured at E and E_0 gives the surface counts N_{ads}. In addition, the solution counts N_{bulk} were recorded at an "infinite" distance between the electrode and the scintillator. With soft β emitters like ^{35}S, a distance of 1 mm is sufficient to eliminate the surface count contribution from the total counts. Therefore only bulk solution counts were measured. Finally, the Gibbs excesses of the adsorbed anions were calculated from the equation

$$\Gamma_- = \frac{N_{ads}}{N_{bulk}} \frac{c_{SO_4^{2-}} 10^{-3} N_A}{R\mu f_b \exp(-\mu x)} \quad (2)$$

where N_A is the Avogadro's constant, $c_{SO_4^{2-}}$/mol l^{-1} is the bulk concentration, μ is the absorption coefficient for ^{35}S radiation (251 cm^{-1} using a formula derived by Lerch [19] and experimental data published by Suttle and Libby [20]), $f_b = 1.86$ [21] is the backscattering factor for gold and R is the roughness factor which is taken as unity for the flame-annealed electrode. It should be stressed that Γ_- measured by the radiochemical technique is the sum of the Gibbs excesses of the SO_4^{2-} and HSO_4^- ions. Therefore we emphasize that both the thermodynamic method based on eqn. (1) and the radiochemical technique give the same physical quantity.

3. Results

The character of SO_4^{2-} adsorption was initially investigated qualitatively with the help of cyclic voltammetry and differential capacity measurements. Figure 1 shows CVs recorded at the Au(111) electrode in a sulphate-free 0.1 M $HClO_4$ solution and in 0.1 M $HClO_4 + 5 \times 10^{-4}$ M K_2SO_4. (For comparison with radiochemical measurements most of the results are presented for the 0.1 M $HClO_4$ supporting electrolyte solution.) The shape of these curves is in good agreement with the data reported in the literature [2,4,5,8]. The inset to Fig. 1 shows the differential capacity curves for the sulphate-free $HClO_4$ solution and with the addition of SO_4^{2-} ions. The adsorption of SO_4^{2-} causes a significant increase in the electrode capacity at $E > 0.2$ V/SCE which is seen as either a sharp peak

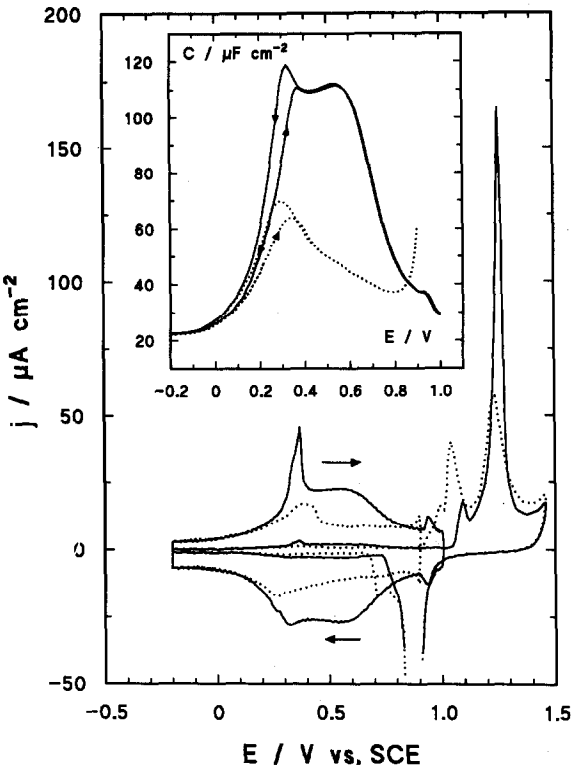

Fig. 1. CVs recorded at an Au(111) electrode in 0.1 M $HClO_4$ (·····) and 0.1 M $HClO_4 + 5 \times 10^{-4}$ M K_2SO_4 solution (———) at a sweep rate of 20 mV s^{-1}. The expanded (20×) double-layer sections of the CVs were recorded using a sweep rate of 10 mV s^{-1}. The inset shows the corresponding differential capacities determined using an ac perturbation of frequency 25 Hz and amplitude 5 mV r.m.s. at a sweep rate of 5 mV s^{-1}.

and a shoulder on the expanded section of the CV or as two peaks on the differential capacity curves. The small reversible peaks seen on the CV at $E \approx 0.93$ V/SCE indicate formation of an ordered SO_4^{2-} overlayer [8]. In addition, sulphate adsorption shifts the oxide formation peaks towards more positive potentials and causes a significant distortion of their shape. Both the CVs and the differential capacities display hysteresis between the curves recorded during the positive-going and negative-going sweeps. Therefore these data cannot be used to determine the amount of adsorbed sulphate.

The potential-step experiments were performed for the supporting electrolyte and for 10 concentrations of K_2SO_4 to measure the charge density at the metal surface corresponding to the equilibrium adsorption of sulphate ions. Figure 2 shows the family of σ_M versus E plots. The charge density plots recorded in the presence of SO_4^{2-} display three inflections. The positions of the inflections correspond to the potentials at which the peaks on the respective CVs or differential capacity curves are seen. The apparent change in the

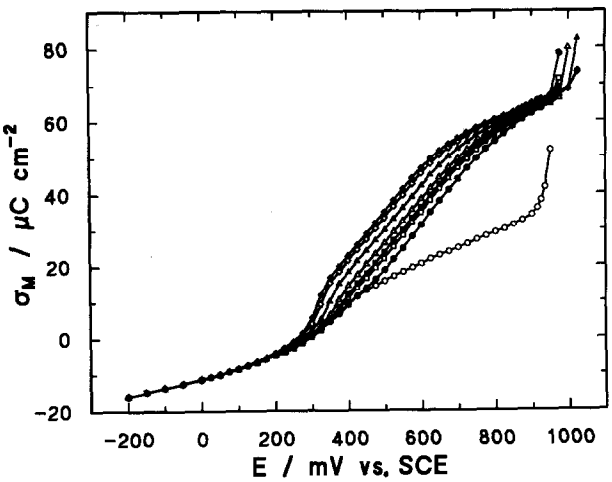

Fig. 2. Charge density–electrode potential curves at the Au(111) electrode for the 0.1 M $HClO_4$ solution (○) with the following additions of K_2SO_4: ● 5×10^{-6} M K_2SO_4; □ 2.5×10^{-5} M K_2SO_4; ■ 5×10^{-5} M K_2SO_4; △ 10^{-4} M K_2SO_4; ▲ 5×10^{-4} M K_2SO_4; ◇ 2.5×10^{-3} M K_2SO_4; ♦ 5×10^{-3} M K_2SO_4. For clarity only the data for a few concentrations are shown in the figure.

slope of the σ_M vs. E plots seen at $E > 600$ mV is also consistent with the decrease in the differential capacity observed in Fig. 1 in the same potential range. The shapes of the curves are invariant with K_2SO_4 concentration. However, their position is shifted along the potential axis. The magnitude of this shift is shown in Fig. 3 where the values of the electrode potential corresponding to selected charge densities (30 μC cm^{-2} and 40 μC cm^{-2} which corresponds to the middle of the σ_M vs. E curve) are plotted against the logarithm of sulphate ion concentration. For comparison, similar

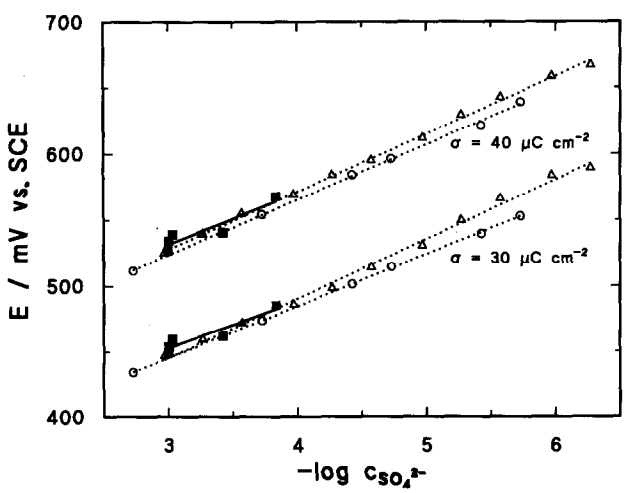

Fig. 3. Esin–Markov plots for two selected charge densities of the Au(111) electrode and the following electrolyte solutions: △ ····· △ 0.1 M $HClO_4 + x$ M K_2SO_4; ○ ····· ○ 0.05 M $KClO_4 + 0.02$ M $HClO_4 + x$ M K_2SO_4; ■ ——— ■ x M $HClO_4 + (0.07 - x)$ M $KClO_4 + 10^{-3}$ M K_2SO_4.

plots determined from the series of measurements in 0.05 M $KClO_4$ + 0.02 M $HClO_4$ as the supporting electrolyte are also included in this figure. The agreement between the two sets of measurements is very good.

At pH ≤ 2 a solution of K_2SO_4 is a mixture of SO_4^{2-} and HSO_4^- ($K_a(HSO_4^-) \approx 1.2\times10^{-2}$). Consequently, adsorption of both SO_4^{2-} and HSO_4^- was assumed in the derivation of eqn. (1) (see Appendix A). In reality one of the two ions may be predominantly adsorbed at the gold electrode. For example, predominant adsorption of HSO_4^- at Au electrodes has been postulated [6,8]. In fact, the plots shown in Fig. 3 can be used to identify the species adsorbed at the metal surface. The slope of the plots in Fig. 3 is equal to the Esin–Markov coefficient given by (see Appendix A, eqn. (A14))

$$\frac{1}{RT}\left(\frac{\partial E}{\partial \ln c_{SO_4^{2-}}}\right)_{\sigma_M} = -\left[\frac{\partial(\Gamma_{SO_4^{2-}} + \Gamma_{HSO_4^-})}{\partial\sigma_M}\right]_{\ln c_{SO_4^{2-}}} \quad (3)$$

In the case of anion adsorption the derivative of the Gibbs excess with respect to the charge density is always positive. Consequently, at a constant charge density the electrode potential shifts in the negative direction with the bulk ion concentration as shown in Fig. 3.

In the experiments described above the $HClO_4$ concentration was kept constant. Under this condition the species concentrations of HSO_4^- and SO_4^{2-} changed in the same direction when the total concentration of K_2SO_4 varied. In fact, adsorption of either SO_4^{2-} or HSO_4^- could cause the negative shift of E at a constant σ_M as observed in Fig. 3. Therefore complementary measurements of the charge densities were performed for a series of solutions with a constant K_2SO_4 concentration and a constant ionic strength, but variable pH. Figure 4 shows the charge density versus potential plots determined in 1×10^{-3} M $K_2SO_4 + x$ M $HClO_4 + (0.07 - x)$ M $KClO_4$ solutions. The bulk concentration of SO_4^{2-} varied between ca. 1×10^{-3} M and 1.5×10^{-4} M and that of HSO_4^- changed from 1×10^{-5} M to 8.5×10^{-4} M by varying the perchloric acid concentration from zero to 0.07 M. In such an electrolyte the expression for the Esin–Markov coefficient has the form (see Appendix B, eqn. (B14))

$$\frac{1}{RT}\left(\frac{\partial E}{\partial \ln c_{SO_4^{2-}}}\right)_{\sigma_M} = -\left\{\frac{\partial\left[\Gamma_{SO_4^{2-}} - (K_a/c_{H^+})\Gamma_{HSO_4^-}\right]}{\partial\sigma_M}\right\}_{\ln c_{SO_4^{2-}}} \quad (4)$$

which is apparently different from the expression derived for a solution which has a constant acid concen-

tration. To discuss the differences between eqns. (3) and (4) two limiting cases can be distinguished.

(i) The predominantly adsorbed species is the SO_4^{2-} ion. In this case the $\Gamma_{HSO_4^-}$ terms in eqns. (3) and (4) can be neglected and then these relations give an identical expression for the Esin–Markov coefficient:

$$\frac{1}{RT}\left(\frac{\partial E}{\partial \ln c_{SO_4^{2-}}}\right)_{\sigma_M} = -\left(\frac{\partial \Gamma_{SO_4^{2-}}}{\partial \sigma_M}\right)_{\ln c_{SO_4^{2-}}} \quad (5)$$

(ii) The predominantly adsorbed species is the HSO_4^- ion. Now the $\Gamma_{SO_4^{2-}}$ terms can be neglected, and the Esin–Markov coefficient for the solution which has a constant acid concentration can be expressed as

$$\frac{1}{RT}\left(\frac{\partial E}{\partial \ln c_{SO_4^{2-}}}\right)_{\sigma M} = -\left(\frac{\partial \Gamma_{HSO_4^-}}{\partial \sigma_M}\right)_{\ln c_{SO_4^{2-}}} \quad (6)$$

whereas for a solution which has a variable acid concentration it has the form

$$\frac{1}{RT}\left(\frac{\partial E}{\partial \ln c_{SO_4^{2-}}}\right)_{\sigma_M} = \frac{K_a}{c_{H^+}}\left(\frac{\partial \Gamma_{HSO_4^-}}{\partial \sigma_M}\right)_{\ln c_{SO_4^{2-}}} \quad (7)$$

In summary, if SO_4^{2-} is the predominantly adsorbed species then identical slopes of E vs. ln $c_{SO_4^{2-}}$ plots at constant σ_M should be observed in experiments performed with constant and variable acid concentrations. In contrast, if HSO_4^- is the adsorbed species, then the two series of measurements should give different E vs. ln $c_{SO_4^{2-}}$ plots with slopes having opposite sign. Therefore the two limiting cases can be easily distinguished. The plots shown in Fig. 4 shift in the negative direction with decreasing acid concentration in the solution, suggesting that SO_4^{2-} is the adsorbed species. To assess this shift quantitatively the values of E corresponding to σ_M values of 30 and 40 $\mu C\ cm^{-2}$ were plotted against log $c_{SO_4^{2-}}$ in Fig. 3 (full squares). They fit very well the correlation determined earlier from experiments performed at a constant acid concentration. This result is consistent with the limiting case (i) and indicates that SO_4^{2-} is the predominantly adsorbed species.

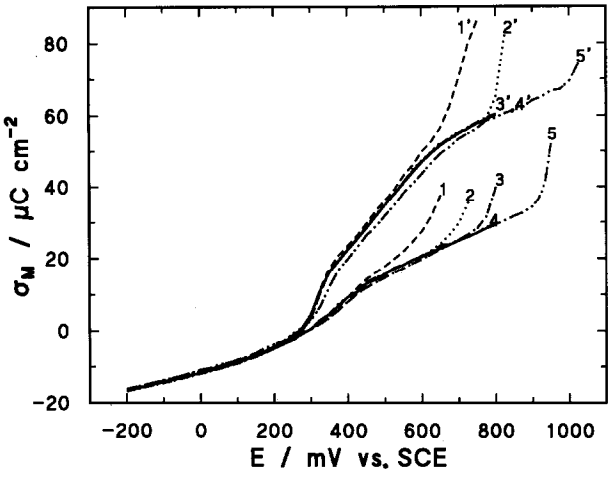

Fig. 4. Plots of charge density vs. electrode potential determined for the Au(111) electrode in solutions of variable acid concentration: ——— 0.07 M $KClO_4$ (curves 1 and 1'); ····· 0.0699 M $KClO_4$ + 1 $\times 10^{-4}$ M $HClO_4$ (curves 2 and 2'); ·—·—· 0.069 M $KClO_4$ + 1 $\times 10^{-3}$ M $HClO_4$ (curves 3 and 3'); ——— 0.05 M $KClO_4$ + 0.02 M $HClO_4$ (curves 4 and 4'); ··—···—·· 0.07 M $HClO_4$ (curves 5 and 5'). Curves 1–5 were obtained in the absence of K_2SO_4; curves 1'–5' were obtained with the addition of 1×10^{-3} M K_2SO_4.

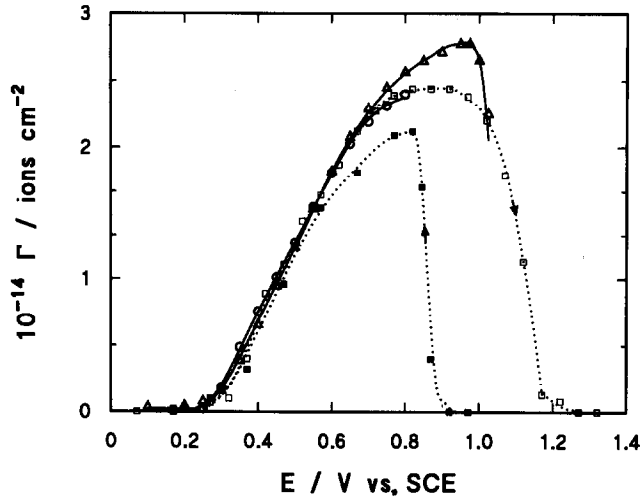

Fig. 5. Gibbs excess vs. electrode potential for SO_4^{2-} adsorption at the Au(111) electrode determined from chronocoulometric experiments in a 0.05 M $KClO_4$ + 0.02 M $HClO_4$ + 5×10^{-4} M K_2SO_4 solution (○); chronocoulometric experiments in 0.1 M $HClO_4$ + 5×10^{-4} M K_2SO_4 (△); radiochemical experiments with the electrode potential progressively changed in the positive direction (□) and radiochemical experiments with the potential changed in the negative direction in a 0.1 M $HClO_4$ + 5×10^{-4} M H_2SO_4 solution (■).

The charge density plots were integrated to give the relative value of the interfacial tension. Next, the Gibbs excess of the adsorbed SO_4^{2-} was calculated by differentiating the interfacial tension with respect to ln $c_{K_2SO_4}$. Figure 5 shows plots of the Gibbs excess versus the electrode potential determined in a 5×10^{-4} M K_2SO_4 solution for the two supporting electrolytes. For comparison, the Gibbs excesses determined from the radiochemical experiments are also included in this diagram. The data show excellent agreement between the Gibbs excesses determined from the thermodynamic analysis of the charge density data and the Gibbs excesses measured using radiotracers.

The thermodynamic analysis can be applied only to the charge density data determined in the double-layer region of the current–potential characteristics of the gold electrode. Therefore measurements of the Gibbs

excesses for SO_4^{2-} using this technique were terminated just before the onset of gold oxide formation. In contrast, the radiochemical method can be used to measure $\Gamma_{SO_4^{2-}}$ even in the presence of the oxide formation reaction (or any other parallel faradaic process.) The measurements of $\Gamma_{SO_4^{2-}}$ were therefore extended up to $E = 1.35$ V. However, the oxide formed at $E > 1.0$ V displaces SO_4^{2-} from the gold surface and the Gibbs excess drops to zero at $E \approx 1.3$ V. When the direction of the applied potential is reversed at $E = 1.35$ V, $\Gamma_{SO_4^{2-}}$ continues to be equal to zero until $E \approx 0.9$ V, i.e. until the onset of oxide reduction. When oxide reduction is completed, $\Gamma_{SO_4^{2-}}$ increases to a value only slightly smaller than $\Gamma_{SO_4^{2-}}$ recorded by starting the data acquisition at $E = 0$ V and moving the potential in the positive direction. The hysteresis seen on the Γ vs. E plots at the positive end of the applied polarizations is caused entirely by the irreversibility of the oxidation–reduction processes of the gold surface.

We have already emphasized that the quantity measured by both the electrochemical and radiochemical techniques is the Gibbs excess. This is the total Gibbs excess of SO_4^{2-} ions present in the interfacial region and is equal to the sum of the Gibbs excess of SO_4^{2-} present in the diffuse and the inner parts of the double layer. Radiochemical measurements do not provide information about the location of the Gibbs excess in the interfacial region. Hence a non-adsorbing electrolyte ($HClO_4$ and $KClO_4$ in the present case) must be used and it is assumed that the Gibbs excess of SO_4^{2-} in the diffuse layer is negligible so that the measured $\Gamma_{SO_4^{2-}}$ corresponds to the specifically adsorbed anions. In contrast, the electrochemical experiments give both the charge density at the metal surface and the total Gibbs excess for the adsorbed anion. Therefore the diffuse-layer theory can be used either to verify that the contribution of the diffuse layer to the measured Gibbs excess is negligible or to calculate the diffuse layer component of the total Gibbs excess.

This point is illustrated in Fig. 6 where the charge density at the metal surface and the absolute value of the charge corresponding to the measured Gibbs excess ($|z_-|F\Gamma_{SO_4^{2-}}$ where $|z_-| = 2$) are plotted against the electrode potential for a 5×10^{-4} M K_2SO_4 + 0.05 M $KClO_4$ + 0.02 M $HClO_4$ solution. These data show that the absolute value of the charge of adsorbed SO_4^{2-} is much larger than the charge on the metal. Therefore adsorption of SO_4^{2-} has a superequivalent character. Under this condition the electric field in the diffuse part of the double layer has a negative sign even at the positively charged metal surface. The diffuse layer is primarily populated by the positive ions and hence the Gibbs excess for anions in the diffuse layer is negative. Since the bulk concentration of SO_4^{2-} is very low, the

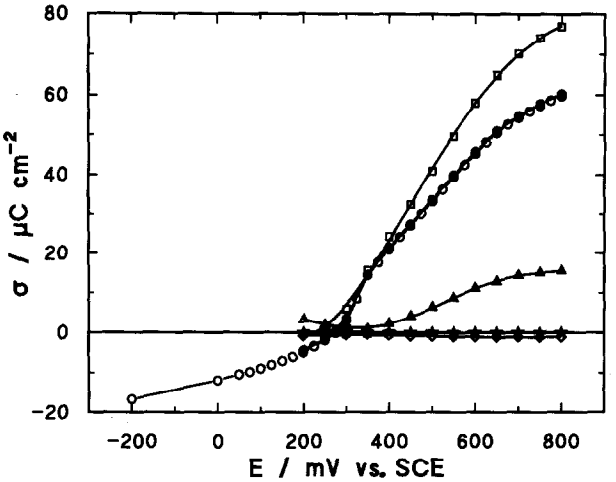

Fig. 6. Charge density versus electrode potential plots for an Au(111) electrode in a 0.05 M $KClO_4$ + 0.02 M $HClO_4$ + 5×10^{-4} M K_2SO_4 solution: ○ charge density σ_M at the metal; □ charge corresponding to the measured Gibbs excess of SO_4^{2-} ion ($|z_-|F\Gamma_{SO_4^{2-}}$ where $|z_-| = 2$); △ charge corresponding to the Gibbs excess of cations (H^+ and K^+) in the diffuse layer ($z_+F\Gamma_+^{2-s}$); ◇ charge corresponding to the Gibbs excess of ClO_4^- in the diffuse layer ($|z_-|F\Gamma_{ClO_4^-}^{2-s}$ with $|z_-| = 1$); ⋆ charge corresponding to the Gibbs excess of SO_4^{2-} in the diffuse layer ($|z_-|F\Gamma_{SO_4^{2-}}^{2-s}$ with $|z_-| = 2$); ● absolute values of net charge density in solution ($|z_-|F\Gamma_{SO_4^{2-}} + |z_-|F\Gamma_{SO_4^{2-}}^{2-s} + |z_-|F\Gamma_{ClO_4^-}^{2-s} - |z_+|F\Gamma_+^{2-s}$).

absolute value of its Gibbs excess in the diffuse layer must be negligible compared with the measured Gibbs excess. In conclusion, the measured Gibbs excess corresponds to the specifically adsorbed sulphate ions.

The validity of this conclusion can be further tested by calculating the charges due to the Gibbs excesses of cations ($z_+F\Gamma_+^{2-s}$ where $z_+ = 1$), perchlorate ion ($|z_-|F\Gamma_{ClO_4^-}^{2-s}$ where $|z_-| = 1$) and sulphate ion ($|z_-|F\Gamma_{SO_4^{2-}}^{2-s}$ where $|z_-| = 2$) in the diffuse part of the double layer using the formula for mixed electrolytes derived by Joshi and Parsons [22]:

$$\Gamma_i^{2-s} = \pm\left(\frac{\epsilon}{2RT}\right)^{1/2} \times \int_{\phi_2}^{0} \frac{c_i^b[\exp(-z_iF\phi/RT) - 1]}{\left\{\sum_i c_i^b[\exp(-z_iF_\phi/RT) - 1]\right\}^{1/2}} d\phi \quad (8)$$

where the lower integration constant ϕ_2 can be determined from [15]

$$(\sigma_M - 2F\Gamma_{SO_4^{2-}}) = \pm(2RT\epsilon)^{1/2}\left\{\sum_i c_i^b\left[\exp\left(\frac{-z_iF}{RT}\phi_2\right) - 1\right]\right\}^{1/2} \quad (9)$$

In eqns. (8) and (9), ϕ and ϕ_2 are the inner potentials at a point within the diffuse layer and at the location of the outer Helmholtz plane respectively, c_i^b is the bulk

concentration of ion i, z_i is the ion valency and ϵ is the dielectric permittivity of the solvent. The calculated charges corresponding to the Gibbs excess of ionic species in the diffuse layer are plotted against the electrode potential in Fig. 6. Since the absolute values of the ionic valency $|z_i|$ were used to calculate the ionic charges, the sign of the charge is determined by the sign of the corresponding Gibbs excess. The results show that the charge of SO_4^{2-} present in the diffuse layer is negligible in comparison with the charge corresponding to the measured Gibbs excess.

4. Summary

Chronocoulometry and radiochemistry were used to study SO_4^{2-} adsorption at the Au(111) electrode. Very good agreement between the Gibbs excesses determined from chronocoulometric and radiochemical measurements was observed. This agreement is an important verification of the reliability of these two in-situ techniques for measuring surface coverages. Although the two techniques give the same physical quantity, which is the Gibbs excess of adsorbed ions, each of them probes different properties of the interface and therefore has different limitations.

The quantity measured by chronocoulometry is the electrode charge density. The surface concentration is calculated from σ_M employing one integration step and one differentiation step and assuming the validity of the electrocapillary equation. Therefore the chronocoulometric technique can be applied only within the double-layer region of the gold electrode. However, since both the Gibbs excess and the charge density are measured simultaneously, this technique provides not only the surface coverages but also an additional electrical variable needed for the interpretation of the coverage data. In contrast, radiochemistry provides information about the Gibbs excess from direct counts of the radioactivity when the electrode with adsorbed radiolabelled material is pressed against the scintillator window. Therefore this technique can be used to study adsorption on both reactive and non-reactive materials. However, the technique is restricted by the efficiency in squeezing out the solution containing radioactive species from the thin layer between the electrode surface and the scintillator window. When the count rates from solution trapped in that gap are high with respect to surface counts, the adsorption measurements are difficult and ultimately become impossible to conduct. In fact, the method cannot be employed for adsorption measurements when the bulk concentration of labelled solute is higher than 10^{-2} M [1]. In addition, the radiochemical technique provides information about the Gibbs excess only.

Acknowledgements

The authors thank Dr. O.M. Magnussen for sending a preprint of ref. 8 prior to publication. This work was supported by grants from the Natural Sciences and Engineering Research Council of Canada and by US Department of Energy, grant DE-AC102-76ER 01198, administered by the Materials Research Laboratory at the University of Illinois.

References

1 J. Lipkowski, L. Stolberg, S. Morin, D.E. Irish, P. Zelenay, M. Gamboa and A. Wieckowski, J. Electroanal. Chem., 355 (1993) 147.
2 D.A. Scherson and D.M. Kolb, J. Electroanal. Chem., 176 (1984) 353.
3 M.S. Zei, D. Scherson, G. Lehmpfuhl and D.M. Kolb, J. Electroanal. Chem., 229 (1987) 99.
4 H. Angerstein-Kozlowska, B.E. Conway, A. Hamelin and L. Stoicoviciu, Electrochim. Acta, 31 (1986) 1051.
5 H. Angerstein-Kozlowska, B.E. Conway, A. Hamelin and L. Stoicoviciu, J. Electroanal. Chem., 228 (1987) 429.
6 P. Zelenay, L.M. Rice-Jackson and A. Wieckowski, J. Electroanal. Chem., 283 (1990) 389.
7 M.S. Zei, G. Qiao, G. Lehmpfuhl and D.M. Kolb, Ber. Bunsenges. Phys. Chem., 91 (1987) 349.
8 O.M. Magnussen, J. Hageböck, J. Hotlos and R.J. Behm, Faraday Discuss. Chem. Soc., (1992) 94.
9 D.M. Kolb, Z. Phys. Chem. NF, 154 (1987) 179.
10 O.M. Magnussen, J. Hotlos, R.J. Nichols, D.M. Kolb and R.J. Behm, Phys. Rev. Lett., 64 (1990) 2929.
11 L. Blum, H.D. Abruña, J. White, J.G. Gordon II, G.L. Borges, M.G. Samant and O.R. Melroy, J. Chem. Phys., 85 (1986) 6732.
12 A. Tadjeddine, D. Guay, M. Ladouceur and G. Tourillon, Phys. Rev. Lett., 66 (1991) 2235.
13 T. Hochiya, H. Honobo and K. Itaya, J. Electroanal. Chem., 315 (1991) 275.
14 J. Richer and J. Lipkowski, J. Electrochem. Soc., 133 (1986) 121.
15 J. Clavilier, J. Electroanal. Chem., 107 (1980) 211.
16 A. Wieckowski, J. Electrochem. Soc., 122 (1975) 252.
17 R. Parsons, Proc. R. Soc. London, Ser. A, 261 (1961) 79.
18 CRC Handbook of Chemistry and Physics (63rd edn.), CRC Press, Boca Raton, FL, 1983.
19 P. Lerch, Helv. Phys. Acta, 26 (1953) 663.
20 A.D. Suttle and W.F. Libby, Anal. Chem., 6 (1955) 921.
21 L.R. Zumwalt, Absolute Beta Counting Using End-Window Geiger-Müller Counters and Experimental Data on Beta Particle Scattering AECV-567, US Atomic Energy Commission Technical Information Service, Oak Ridge, TN, 1976.
22 K.M. Joshi and R. Parsons, Electrochim. Acta, 4 (1961) 129.
23 H.D. Hurwitz, J. Electroanal. Chem., 10 (1965) 35.
24 E. Dutkiewicz and R. Parsons, J. Electroanal. Chem., 11 (1966) 100.
25 S. Lakshmanan and S.K. Rangarajan, J. Electroanal. Chem., 27 (1970) 127.
26 S. Lakshmanan and S.K. Rangarajan, J. Electroanal. Chem., 27 (1970) 170.
27 W.R. Fawcett and T.A. McCarrick, J. Electrochem. Soc., 123 (1976) 1325.
28 E.A. Guggenheim, Philos. Mag., 19 (1935) 588.

Appendix A

Consider adsorption of SO_4^{2-} and HSO_4^- from a solution of a mixed electrolyte without a common ion such as 0.1 M $HClO_4 + x$ M K_2SO_4, where x varies between 5×10^{-6} M and 5×10^{-3} M. The concentration of $HClO_4$ is much higher than the concentration of K_2SO_4, and hence any change in the concentration of K_2SO_4 has a negligible effect on the ionic strength of the solution. Since K_2SO_4 dissociates to form predominantly HSO_4^- in a 0.1 M $HClO_4$ solution, the solution behaves as a mixture of two 1:1 electrolytes ($HClO_4$ and $KHSO_4$). For the highest K_2SO_4 concentration employed in these measurements, the ionic strength of the solution is only 5% higher than the ionic strength of the pure 0.1 $HClO_4$. Effectively, the adsorption of SO_4^{2-} and HSO_4^- takes place from a solution of constant ionic strength and constant acid activity (concentration). However, a distinction has to be made between the present case and the frequently discussed case of adsorption from a mixed electrolyte solution with constant ionic strength formed by two salts with a common cation [23–27]. Therefore we shall refer to the present case as adsorption from a solution with an excess of supporting electrolyte. The electrocapillary equation for a gold electrode in contact with the mixed electrolyte solution may be written as

$$-\mathrm{d}\gamma = -\frac{\sigma_M}{F}\mathrm{d}\bar{\mu}_e(\mathrm{Au}) + \Gamma_{H^+}\,\mathrm{d}\bar{\mu}_{H^+} + \Gamma_{K^+}\,\mathrm{d}\bar{\mu}_{K^+} + \Gamma_{ClO_4^-}\,\mathrm{d}\bar{\mu}_{ClO_4^-} + \Gamma_{HSO_4^-}\,\mathrm{d}\bar{\mu}_{HSO_4^-} + \Gamma_{SO_4^{2-}}\,\mathrm{d}\bar{\mu}_{SO_4^{2-}} + \Gamma_{H_2O}\,\mathrm{d}\mu_{H_2O} \quad \text{(A1)}$$

We can reasonably assume that, in the presence of an excess of supporting electrolyte, the variation of K_2SO_4 concentration has a negligible effect on the activity of water and hence the last term in eqn. (A1) can be neglected. In addition, the following conditions should be taken into consideration.

(i) The electrochemical potentials of HSO_4^- and SO_4^{2-} are related through the acid dissociation equilibrium $HSO_4^- + H_2O = H_3O^+ + SO_4^{2-}$:

$$\mu_{H_2O} + \bar{\mu}_{HSO_4^-} = \bar{\mu}_{H_3O^+} + \bar{\mu}_{SO_4^{2-}} \quad \text{(A2)}$$

and hence

$$\mathrm{d}\bar{\mu}_{HSO_4^-} = \mathrm{d}\bar{\mu}_{H_3O^+} + \mathrm{d}\bar{\mu}_{SO_4^{2-}} \quad \text{(A3)}$$

since μ_{H_2O} remains constant as there is a large excess of water.

(ii) The chemical potential of an ionic species can be expressed as

$$\mu_i = \mu_i^\circ + RT \ln c_i\gamma_i \quad \text{(A4)}$$

where c_i is the species concentration of an ion i and γ_i is the activity coefficient of ion i. We can use Guggenheim's expression for the single-ion activity coefficient [28]

$$\ln \gamma_i = -Az_i^2\frac{\sqrt{I}}{1+\sqrt{I}} + \sum_j \beta_{ij}c_j \quad \text{(A5)}$$

to assess the variation of the activity coefficient with changing K_2SO_4 concentration. In eqn. (A5) is the Debye–Hückel constant, β_{ij} is the interaction coefficient between ion i and the counter-ion j and z_i is the valency of ion i. The 5% change in the ionic strength due to moving from a pure 0.1 M $HClO_4$ to 0.1 M $HClO_4 + 5 \times 10^{-3}$ M K_2SO_4 solution would cause the first term of eqn. (A5) to change by 1.8% only. The interaction coefficients β_{ij} are of the order of 0.1 [26]. Hence the second term of eqn. (A5) should vary by no more than 1×10^{-3} when the concentration of K_2SO_4 varies between zero and 5×10^{-3} M. Such changes are negligible, and hence the activity coefficient can be considered as independent of the K_2SO_4 concentration. The change of the chemical potential of an ion i can then be written as

$$\mathrm{d}\mu_i = RT\ \mathrm{d}\ln c_i \quad \text{(A6)}$$

and for a constant acid concentration $\mathrm{d}\mu_{H^+} = \mathrm{d}\mu_{ClO_4^-} = 0$.

If we eliminate the electrochemical potentials and use conditions (A3) and (A6), we can write the electrocapillary equation in the form

$$-\mathrm{d}\gamma = \sigma_M\,\mathrm{d}E_{H^+} + \Gamma_{-}RT\,\mathrm{d}\ln c_{SO_4^{2-}} + \Gamma_{K^+}RT\,\mathrm{d}\ln c_{K^+} \quad \text{(A7)}$$

where $\Gamma_- = \Gamma_{SO_4^{2-}} + \Gamma_{HSO_4^-}$. Further, in an electrolyte of constant H_3O^+ activity $\mathrm{d}E_{H^+} = \mathrm{d}E$, where E is the potential of the gold electrode with respect to an external reference electrode (SCE in the present work). The following arguments can also be made to show that the last term of eqn. (A7) is negligible in comparison with the second term. In the presence of 0.1 M $HClO_4$ in the solution, the concentration of HSO_4^- is about 10 times larger than the concentration of SO_4^{2-} (K_a (HSO_4^-) $= 1.2 \times 10^{-2}$). Hence, to a good approximation we can write

$$c_{HSO_4^-} \approx c_{K_2SO_4} = 0.5c_{K^+} \quad \text{(A8)}$$

where $c_{K_2SO_4}$ is the total concentration of K_2SO_4 in the solution investigated. Using conditions (A3) and (A6) we obtain

$$\mathrm{d}\ln c_{HSO_4^-} = \mathrm{d}\ln c_{SO_4^{2-}} \approx \mathrm{d}\ln c_{K_2SO_4} = \mathrm{d}\ln c_{K^+} \quad \text{(A9)}$$

Next we shall use the electroneutrality condition to estimate the relative magnitude of Γ_- and Γ_{K^+}:

$$2\Gamma_{SO_4^{2-}} + \Gamma_{HSO_4^-} - \sigma_M/F = \Gamma_{H^+} + \Gamma_{K^+} \quad \text{(A10)}$$

We assume that cations H_3O^+ and K^+ are present in the diffuse part of the double layer only (a very good approximation), and then it follows that

$$\frac{\Gamma_{K^+}}{\Gamma_{H^+}} = \frac{c_{K^+}}{c_{H_3O^+}} \quad \text{(A11)}$$

Since $c_{H_3O^+} \gg c_{K^+}$ the Gibbs excess of K^+ is negligible in comparison with Γ_{H^+}. Sulphate adsorbs strongly on gold, and at most of the potentials investigated its adsorption has a superequivalent character so that $2\Gamma_{SO_4^{2-}} + \Gamma_{HSO_4^-} > \Gamma_{H^+}$. This condition indicates that $\Gamma_{SO_4^{2-}} + \Gamma_{HSO_4^-} \gg \Gamma_{K^+}$. The electrocapillary equation can than be written in a simple form:

$$-d\gamma = \sigma_M \, dE + \Gamma_- RT \, d \ln c_{SO_4^{2-}} \quad \text{(A12)}$$

Using Parsons function $\xi = \gamma + \sigma_M E$ we can change the independent electrical variable [17]:

$$-d\xi = E \, d\sigma_M + \Gamma_- RT \, d \ln c_{SO_4^{2-}} \quad \text{(A13)}$$

Cross-differentiation of eqn. (A13) gives the expression for the Esin–Markov coefficient:

$$\frac{1}{RT}\left(\frac{\partial E}{\partial \ln c_{SO_4^{2-}}}\right)_{\sigma_M} = -\left(\frac{\partial \Gamma_-}{\partial \sigma_M}\right)_{\ln c_{SO_4^{2-}}} \quad \text{(A14)}$$

Appendix B

Consider the adsorption of SO_4^{2-} and HSO_4^- from a solution of a mixed electrolyte such as $(0.07 - x)$ M $KClO_4 + x$ M $HClO_4 + 1 \times 10^{-3}$ M K_2SO_4, where x varies between zero and 0.07. Apparently, the adsorption of SO_4^{2-} and HSO_4^- takes place from a solution of constant K_2SO_4 concentration and constant ionic strength but of variable acid concentration. The electrocapillary equation for a gold electrode in contact with the mixed electrolyte solution is again given by eqn. (A1). If we eliminate the electrochemical potentials it can be written as

$$\begin{aligned} -d\gamma = {} & \sigma_M \, dE_{ClO_4^-} + \Gamma_{K^+} \, d\mu_{KClO_4} + \Gamma_{H^+} \, d\mu_{HClO_4} \\ & + \Gamma_{HSO_4^-}(d\mu_{HSO_4^-} - d\mu_{ClO_4^-}) \\ & + \Gamma_{SO_4^{2-}}(d\mu_{SO_4^{2-}} - 2 \, d\mu_{ClO_4^-}) \end{aligned} \quad \text{(B1)}$$

where the chemical potential of an ionic species i is given by eqn. (A4). In the mixed electrolyte of constant ionic strength the activity coefficient γ_i can be considered as independent of the electrolyte composition and the change in the chemical potential can be expressed in terms of the change in the logarithm of the ion concentration. In fact, eqn. (A5) can be used to justify this point. The activity coefficients can be written for cations as

$$\begin{aligned} \ln \gamma_+ = {} & -Az_+^2 \frac{\sqrt{I}}{1 + \sqrt{I}} + \beta_{+,ClO_4^-} c_{ClO_4^-} \\ & + \beta_{+,HSO_4^-} c_{HSO_4^-} + \beta_{+,SO_4^{2-}} c_{SO_4^{2-}} \end{aligned} \quad \text{(B2)}$$

and for anions as

$$\ln \gamma_- = -Az_-^2 \frac{\sqrt{I}}{1 + \sqrt{I}} + \beta_{-,K^+} c_{K^+} + \beta_{-,H^+} c_{H^+} \quad \text{(B3)}$$

The concentrations of HSO_4^- and SO_4^{2-} are at least two orders of magnitude smaller than the concentration of ClO_4^-. Therefore the last two terms of eqn. (B2) can be neglected in comparison with the second term and $\ln \gamma_+$ can be considered as independent of the electrolyte composition.

The concentrations of the hydronium and potassium ions can be written as $c_{H^+} = 0.07y$ and $c_{K^+} = (1 - y)0.07$ where $y = x/0.07$ varies between zero and unity. The activity coefficient for an anion can then be expressed in the following form:

$$\begin{aligned} \ln \gamma_- = {} & -Az_-^2 \frac{\sqrt{I}}{1 + \sqrt{I}} + 0.07\beta_{-,K^+} \\ & + 0.07(\beta_{-,H^+} - \beta_{-,K^+})y \end{aligned} \quad \text{(B4)}$$

The interaction coefficients β are of the order of 0.1 [26,27]. Hence the changes in the last term with the electrolyte composition must have the character of a third-order effect and can be neglected. Therefore expression (B1) can be simplified as follows.

(i) The concentration of the perchlorate ion in the mixed solvent is constant and hence $d\mu_{ClO_4^-} = 0$ and $dE_{ClO_4^-} = dE$, where E is the potential of the gold electrode with respect to an external reference electrode.

(ii) The following arguments can be used to show that the sum of the second and third terms of eqn. (B1) is equal to zero:

$$d\mu_{HClO_4} = RT \, d \ln x \quad \text{(B5)}$$

and

$$\begin{aligned} d\mu_{KClO_4} = {} & RT \, d \ln(0.07 - x) \\ = {} & -RT[x/(0.07 - x)] \, d \ln x \end{aligned} \quad \text{(B6)}$$

Using eqns. (B5) and (B6) the sum of the two terms can be written as

$$\begin{aligned} & \Gamma_{H^+} \, d\mu_{HClO_4} + \Gamma_{K^+} \, d\mu_{KClO_4} \\ & = \{\Gamma_{H^+} - [x/(0.07 - x)]\Gamma_{K^+}\} RT \, d \ln x \end{aligned} \quad \text{(B7)}$$

We can assume further that cations H_3O^+ and K^+ are

present in the diffuse part of the double layer only, and then from eqn. (A11) we obtain

$$\Gamma_{K^+} = [(0.07 - x)/x]\Gamma_{H^+} \tag{B8}$$

When relation (B8) is substituted into (B7) the result is zero. The electrocapillary equation can then be written

$$-d\gamma = \sigma_M\, dE + RT\Gamma_{HSO_4^-}\, d\ln c_{HSO_4^-} + RT\Gamma_{SO_4^{2-}}\, d\ln c_{SO_4^{2-}} \tag{B9}$$

The total concentration of K_2SO_4 is constant during this experiment:

$$c_{SO_4^{2-}} + c_{HSO_4^-} = 1 \times 10^{-3}\text{M} \tag{B10}$$

Hence the change in the logarithm of the HSO_4^- concentration can be expressed as

$$d\ln c_{HSO_4^-} = -(c_{SO_4^{2-}}/c_{HSO_4^-})\, d\ln c_{SO_4^{2-}} \tag{B11}$$

Next, using the acid dissociation equilibrium, the ratio $(c_{SO_4^{2-}}/c_{HSO_4^-})$ can be written as

$$c_{SO_4^{2-}}/c_{HSO_4^-} = K_a(HSO_4^-)/c_{H^+} \tag{B12}$$

Combining equations (B9), (B11) and (B12), the electrocapillary equation can be written in the final form

$$-d\gamma = \sigma_M\, dE + RT\left(\Gamma_{SO_4^{2-}} - \frac{K_a}{c_{H^+}}\Gamma_{HSO_4^-}\right) d\ln c_{SO_4^{2-}} \tag{B13}$$

The following expression for the Esin–Markov coefficient can be derived from eqn. (B13) by changing the independent electrical variable and cross-differentiating:

$$\frac{1}{RT}\left(\frac{\partial E}{\partial \ln c_{SO_4^{2-}}}\right)_{\sigma_M} = -\left\{\frac{\partial\left[\Gamma_{SO_4^{2-}} - (K_a/c_{H^+})\Gamma_{HSO_4^-}\right]}{\partial\sigma_M}\right\}_{\ln c_{SO_4^{2-}}} \tag{B14}$$